ЖУРНАЛ СТРУКТУРНОЙ ХИМИИ

2016. Том 57, № 5 *Июнь – июль* *С. 1026 – 1034*

UDC 541.65(66):546.75:546.21

SONOCHEMICAL AND SOLVOTHERMAL SYNTHESIS OF METHANOL {2-[(2-HYDROXY-1,1-DIMETHYL-ETHYLIMINO)-METHYL]PHENOLATO}DIOXIDO-MOLYBDENUM(VI) COMPLEX AND ITS DECOMPOSITION TO MoO_3 NANOPARTICLES

S. Saeednia[1], P. Iranmanesh[2], M. Hatefi Ardakani[1], N. Ebadinejad[1]

[1]*Department of Chemistry, Faculty of Science, Vali-e-Asr University of Rafsanjan, Rafsanjan, Iran*
E-mail: sami_saeednia@yahoo.com, s.saeednia@vru.ac.ir
[2]*Department of Physics, Faculty of Science, Vali-e-Asr University of Rafsanjan, Rafsanjan, Iran*

Received April, 8, 2015 *Revised — October, 16, 2015*

As a new precursor to prepare nano molybdenum trioxide, methanol {2-[(2-hydroxy-1, 1-dimethyl-ethylimino)-methyl]phenolato}dioxidomolybdenum(VI) complex (**1**) with the Schiff base ligand (H_2L) is synthesized by two different methods: solvothermal and sonochemical. Nanoparticles of **1** are obtained by one-pot solvothermal treatment of methanolic solutions of the ligand and di-oxomolybdenyl acetylacetonate at 150 °C for 24 h and for improving the quality of nanostructures by sonochemical method with two types of solvents, different concentrations of initial reagents and also different sonication times. The thermal stability of nanosized compound **1** is studied by thermal gravimetric (TG) analysis and differential scanning calorimetry (DSC). Nanoparticles of orthorhombic α-MoO_3 are obtained by calcination of nanostructures of compound **1** at 700 °C. All compounds and the obtained molybdenum trioxide nanostructures are characterized by elemental analysis, FT-IR, UV-Vis spectroscopy, X-ray powder diffraction (XRD), and scanning electron microscopy (SEM).

DOI: 10.15372/JSC20160518

K e y w o r d s: nanosized MoO_3, Mo(VI) tridentate Schiff base complex, solvothermal, sonochemical, thermal analysis.

INTRODUCTION

The chemistry of molybdenum has become a prospective area for research. This is due to the molybdenum ability to form compounds with most inorganic and organic ligands, in addition to bi- and polynuclear compounds [1—3]. Molybdenum compounds have many and varied potential applications. An exceptional feature of molybdenum is that it has versatile oxidation states, from –2 to 6, and coordination numbers ranging from 4 to 8 [4]. Molybdenum Schiff base complexes have continued to play the role of one of the most important models of molybdoenzymes due to their preparative accessibility [5, 6]. Schiff bases derived from salicylaldehyde and amino alcohols have been widely used to prepare dioxo molybdenum complexes containing the MoO_2^{2+} core [7, 8]. These ligands having both alcoholic and phenolic hydroxyl groups and also one neutral nitrogen donor (CH=N imino group) can be used as polidentate ligands in molybdenum chemistry [9]. High oxidation states of molybdenum could be dominated by terminally bonded oxo groups of polidentate Schiff base ligands [10].

The reduction of the size of metal complexes to nano scale has been extremely attractive [11, 12]. Sonochemistry is one of the research area in which molecules undergo a chemical reaction due to the application of powerful ultrasound irradiation and many kinds of nanomaterials and nano coordination compounds have been prepared by this method in recent years [13—19].

The investigations on the microstructure of crystalline materials received considerable attention during the last years in connection with the preparation of nanostructured materials. The microstructure influences the properties of materials and can be controlled by different synthesis methods. Transition metal oxides like MoO_3 have numerous industrial applications due to their optical, electrical, and thermal properties [20]. Molybdenum trioxide is an *n*-type semiconductor with a large band gap of 3.2 eV [21]. Generally, molybdenum trioxide is prepared by thermal evaporation [22], electrode deposition [23], flash deposition [24], the sol-gel method [25], or the reactive sputtering method [26].

During these years, almost more efforts have been made in the synthesis of nanoscale particles of metals. In this work, we have been interested in the synthesis of molybdenum trioxide nanoparticles through thermal decomposition of the methanol {2-[(2-hydroxy-1, 1-dimethyl-ethylimino)-methyl]phenolato}dioxidomolybdenum(VI) complex prepared by sonochemical and solvothermal methods. A major interest at the moment is the use of a new coordination compound for the preparation of metal oxide nanoparticles to control nanocrystalline size, shape, and distribution. Herein, we reported the sonochemical and solvothermal methods to produce the Mo(VI) Schiff base complex. The complex was then used as solid precursors to yield pure-phase MoO_3 nanoparticles by thermal decomposition at 700 °C for 1 h. The products were characterized by XRD, FT-IR, UV-Vis spectroscopy, ^{13}C NMR and ^{1}H NMR, TG/DSC analysis, and elemental analysis.

EXPERIMENTAL

Materials and measurements. All the chemicals and solvents employed for synthesis were of analytical grade and used as received without further purification. $[MoO_2(acac)_2]$ was prepared according to the method reported in the literature [27].

FT-IR spectra of the ligand and the complexes were recorded in the 4000—400 cm^{-1} wavenumber range using KBr disks as the standard on a Thermo SCIENTIFIC model NICOLET iS10 spectrophotometer to indicate the chemical bonding. The UV-Vis absorption spectra were obtained by a PG instruments Ltd, T70/T80 series (UV-Vis) spectrometer in the wavelength range 300—800 nm with HPLC grade methanol as a solvent. A Brucker Avance DPX 400 MHz instrument was used to record the NMR spectra with TMS and $CDCl_3$ as the internal standard and the solvent, respectively. The elemental analysis was performed on a LECO, CHNS-932 analyzer. X-ray powder diffraction (XRD) measurements were performed using a Philips X′pert diffractometer with monochromatic CuK_α radiation to investigate the crystal structure and phase identification. The simulated XRD powder pattern based on the single crystal data was obtained using the Mercury software [28]. The nanocompounds were characterized by scanning electron microscopy (SEM) (Philips XL 30). The ultrasonic generator was applied on an ultrasonic bath wiseclean-wvc-A02H (frequency of 50 kHz). Thermogravimetric analysis (TG) and differential scanning calorimetry (DSC) of the title compound were performed on a computer-controlled NETZSCH model PC Luxx 409 apparatus. A single-phased powder sample of **1** was loaded into alumina pans and heated with a ramp rate of 10 °/min from room temperature to 800 °C under an argon atmosphere.

Synthesis of the Schiff base ligand [2-[(2-hydroxy-1,1-dimethyl-ethylimino)-methyl]-phenol] (H_2L). The Schiff base ligand was prepared by the standard methods. The solution of 2-hydroxybenzaldehyde (2 mmol, 0.224 g) was mixed with 2-amino-2-methyl-propan-1-ol (2 mmol, 0.178 g) to prepare H_2L in ethanol (20 ml). The bright yellow solution was stirred and heated to reflux for 1 h. The desired yellow solution was precipitated by mixing with diethyl ether and then filtered off and dried in air. H_2L: Yield: 84%, m.p. = 63—66 °C, selected FT-IR data, ν(cm^{-1}): 3371 (O—H), 2964 (C—H), 1601 (C=N), 1550 (C=C). ^{1}H NMR (δ): 1.31 (s, 6H, 2(CH_3)), 1.96 (br s, aliphatic OH), 3.59 (2H, CH_2), 6.86 (d of tri, ArH, J = 7.2 and J = 0.8 Hz), 6.92 (d, ArH, J = 8 Hz), 7.25—7.32 (m, 2H, ArH), 8.37 (s, 1H, HC=N) and 13.94 (br s, Aromatic OH). ^{13}CNMR (δ): 23.56 (2CH_3), 60.92 ((CH_3)2CCH_2), 71.14(CH_2), 117.34, 118.69, 118.36 131.65, 132.44 and 161.95 (aromatic C), 162.23(HC=N).

Synthesis of methanol {2-[(2-hydroxy-1,1-dimethyl-ethylimino)-methyl]phenolato}dioxidemolybdenum(VI) complex (1). The molybdenum complex was prepared as follows: the Schiff base

Table 1

Experimental conditions to prepare $[MoO_2L(CH_3OH)]$ *by the sonochemical method*

Sample No.	H_2L, mmol	$MoO_2(acac)_2$, mmol	Solvent	Sonication time, min	Observation from SEM images	Size, nm
1	5	5	Methanol/chloform	80	Nanorods (Fig. 5, *a*)	50—60
2	5	2.5	Methanol/chloform	80	Microstructure contains nanorods, nanoplates and nanoparticles	—
3	2.5	2.5	Methanol/chloform	80	Nanorods	180—200
4	2.5	5	Methanol/chloform	80	Nanorods	70—80
5	2.5	2.5	Methanol	80	Agglomerated nanoparticles (Fig. 5, *b*)	30—40
6	5	5	Methanol	80	More agglomerated nanoparticles	40—50
7	2.5	5	Methanol	80	More agglomerated nanoparticles	40—50
8	5	2.5	Methanol	80	More agglomerated nanoparticles	40—50
9	5	5	Methanol/chloform	40	Semi bulk	—
10	2.5	2.5	Methanol	40	Semi bulk	—

ligand, H_2L (1 mmol, 0.399 g,) was dissolved in 20 ml of methanol. After that a methanolic solution of dioxo molybdenyl acetylacetonate (1 mmol, 0.326 g) was added to the first solution and then the reaction mixture was refluxed for 1 h. The yellowish solution was concentrated to yield yellow powder. This powder was washed with warm methanol. $[MoO_2L(CH_3OH)]$ bulk; Yield: 77 %, m.p.: 296. Elemental analysis: calcd. (%) for $C_{12}H_{17}NO_5$ Mo: C 41.04, H 4.88, N 3.99; found: C 40.69, H 5.72, N 3.56. Selected FT-IR data; ν (cm^{-1}): 3215(O—H), 2975 (C—H), 1632 (C=N), 1558 (C=C), 911 and 830 (Mo—O).

Preparation of complex (1) by the solvothermal method. $Mo(acac)_2$ (5 mmol) and the H_2L ligand (5 mmol) were dissolved in 15 ml MeOH. The solution was charged into a Teflon-lined stainless steel autoclave and then heated at 150 °C for 24 h. The product was filtered, dried, and characterized after the autoclave was cooled immediately to room temperature. m.p: 296 °C. FT-IR (KBr disc): 3214, 2974, 1629, 1558, 911, 830 cm^{-1}.

Preparation of complex (1) under ultrasonic irradiation. A solution of 0.5 mmol H_2L Schiff base ligands (25 ml methanol or chloroform) was poured dropwise into a 25 ml methanolic solution of 0.5 mmol dioxo molybdenylacetylacetonate during 40 min under ultrasonic irradiation. After the end of the titration the solution was kept in the ultrasonic bath for a period of 40 min. After that the obtained precipitates were filtered and dried. Yield: 88%. m.p: 296 °C. FT-IR (KBr disc): 3215, 2978, 1629, 1558, 911, 830 cm^{-1}. To study the effect of the type of solvent, the initial reagent concentrations, and the sonication time on the size and morphology of compound **1**, the above processes were carried out under different conditions (Table 1).

Preparation of molybdenum trioxide. Calcination of nanosized complex **1** at 700 °C in a furnace and static air atmosphere for 4 h afforded α-MoO_3 nanoparticles. Selected FT-IR data, ν (cm^{-1}): 995 (Mo=O), 864 (Mo—O—Mo), 567 (Mo_2O_2).

RESULTS AND DISCUSSION

The reaction of 2-[(2-hydroxy-1,1-dimethyl-ethylimino)-methyl]-phenol (H_2L) with dioxo molybdenum acetylacetonate leads to the formation of a methanol {2-[(2-hydroxy-1,1-dimethyl-ethylimino)-methyl]phenolato}dioxidomolybdenum(VI) complex (Scheme 1) [29]. Nanostructures of compound **1** were obtained by ultrasonic irradiation and the solvothermal process, while bulk powder

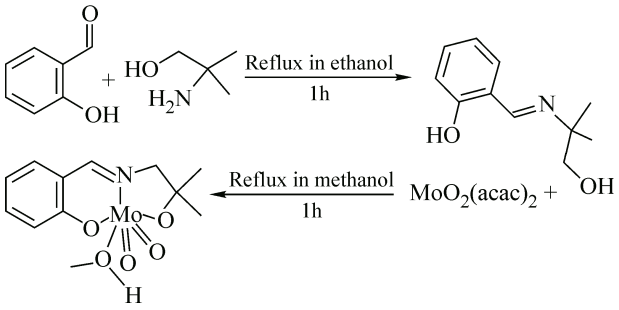

Scheme 1. Preparation of the methanol {2-[(2-hydroxy-1,1-dimethyl-ethylimino)-methyl]phenolato}dioxidomolybdenum(VI) complex

of compound **1** was obtained by reflux of the methanolic solution of the reagents. Scheme 2 gives an overview of the methods used for the synthesis of compound **1** using three different routes.

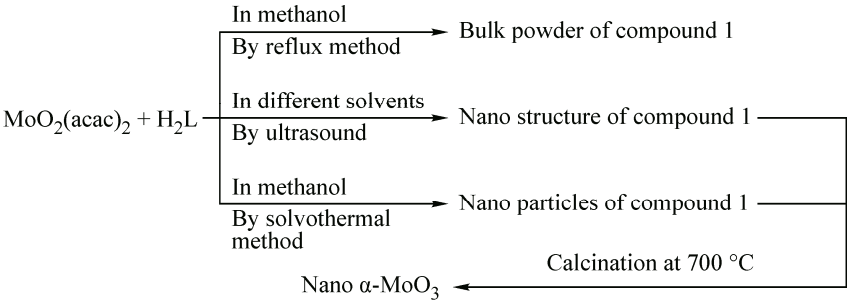

Scheme 2. Material produced and synthetic methods

The FT-IR spectra of the structure produced by the sonochemical and solvothermal methods and of the bulk material produced by the reflux method are indistinguishable (Fig. 1). A comparison of the spectra of the complexes with the ligand provides evidence for the coordination mode of the ligand in the complex. A sharp band appearing at 1601 cm^{-1} due to ν(C=N) (azomethine) shifts towards upper wavenumber at about 1630 cm^{-1}. This indicates the involvement of azomethine nitrogen in the coordination to the metal center. IR spectra of the Mo complexes show two characteristic bands in the regions of 830 and 910 cm^{-1}, which could be assigned to the symmetric and asymmetric stretching vibrations of *cis*-dioxo (MoO_2) respectively [30]. The IR spectra of the molybdenum complexes as bulk and the complex produced by the sonochemical and solvothermal methods are identical.

Fig. 2 shows the simulated XRD pattern from the single crystal X-ray data of compound **1** (Fig. 2, *a*) in comparison with the XRD pattern of the typical sample of compound **1** prepared by the sonochemical process and the solvothermal method (Fig. 2, *b*, *c*). The pattern for the three methods is similar. Acceptable matches, with slight differences in 2θ, were observed between the simulated and experimental powder X-ray diffraction patterns. This indicates that the compounds obtained by the sonochemical and solvothermal processes are identical to that obtained by single crystal diffraction. The significant broadening of the peaks indicates that the particles have nanometer dimensions.

The electronic absorption spectrum of complex **1** was measured in the MeOH solvent in the range 300—800 nm. The electronic spectra of the Schiff base ligand exhibit two maximum peaks at 315 and 400 nm. These peaks are attributed to $\pi\rightarrow\pi^*$ and $n\rightarrow\pi^*$ transitions, respectively (Fig. 3). The first band shifted to 340 nm in the spectra of the complex and the second band $n\rightarrow\pi^*$ disappeared in the spectra of the complex (Fig. 3). After complexation, atoms with lone pairs connect to the central metal and the ligand structure would be rigid. Therefore, electron transfer is not available for these atoms as the $n\rightarrow\pi^*$ transition. The electronic spectra shows that the peak of the $\pi\rightarrow\pi^*$ transition shifted to the highest wavelength after complexation. The aromatic rings of the organic ligands must be rigid after

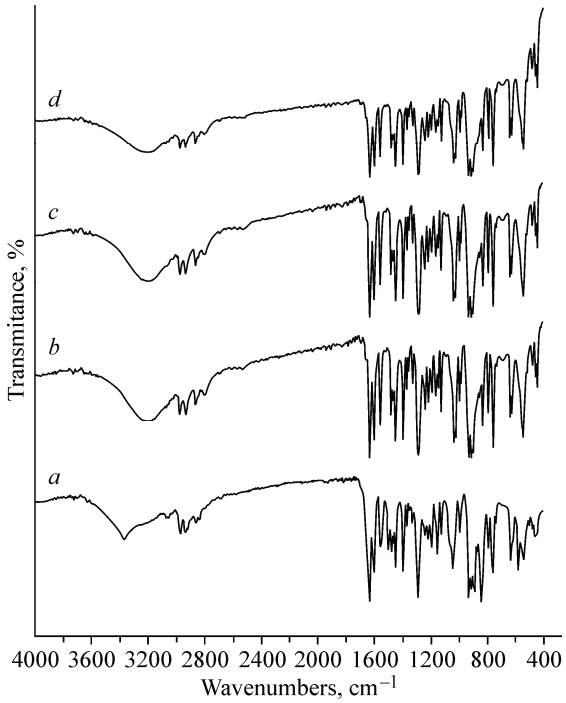

Fig. 1. FT-IR spectra of the ligand (*a*), the bulk complex (*b*), the complex produced by the sonochemical method (*c*), the complex produced by the solvothermal method (*d*)

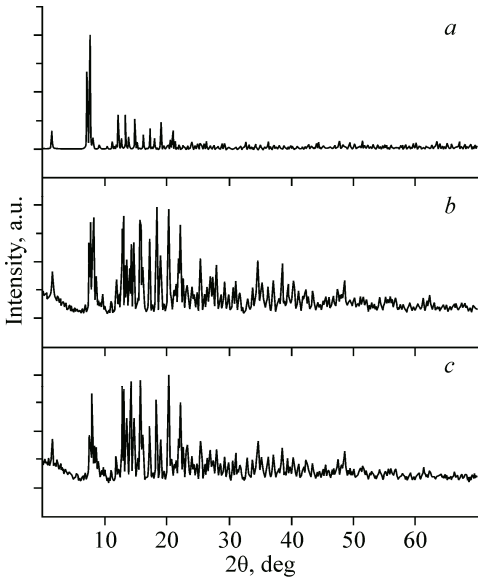

Fig. 2. XRD patterns: simulated pattern based on the single crystal data of compound **1** (*a*), compound **1** prepared by the sonochemical process (*b*) and the solvothermal method (*c*)

the coordination because of π—π stacking interactions. Thus, the electronic energy level of aromatic rings decreased.

The morphology and size of compound **1** are investigated by SEM. Fig. 4 shows the SEM image of compound **1** obtained by the solvothermal method. As seen, some nanoparticles obtained have a diameter of about 50 nm and uniform morphology. No more optimization was made.

Various parameters in the sonochemical process, such as different solvents, concentrations of starting materials, and the sonication time affect the size and morphology of the structures. Experimental conditions to prepare [$MoO_2L(CH_3OH)$] are summarized in Table 1.

Optimization of conditions in the sonochemical process. Type of solvents. For the investigation of the effect of solvents, two types of solvents were used; methanol and a methanol:chloroform mixture. As seen in Fig. 5, *a* and *b*, the type of the solvent affected the morphology and shape of the complex; in 1:1 methanol:chloroform some nanorods were obtained while the use of methanol leads to different structures; some nanoparticles of the complex were obtained.

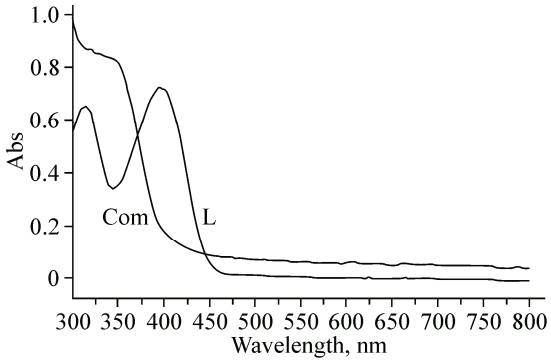

Fig. 3. Electronic spectra of [$MoO_2L(CH_3OH)$] at room temperature (25 °C)

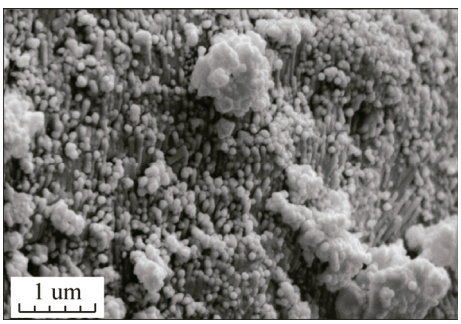

Fig. 4. SEM images of nanoparticles of compound **1** obtained by the solvothermal method

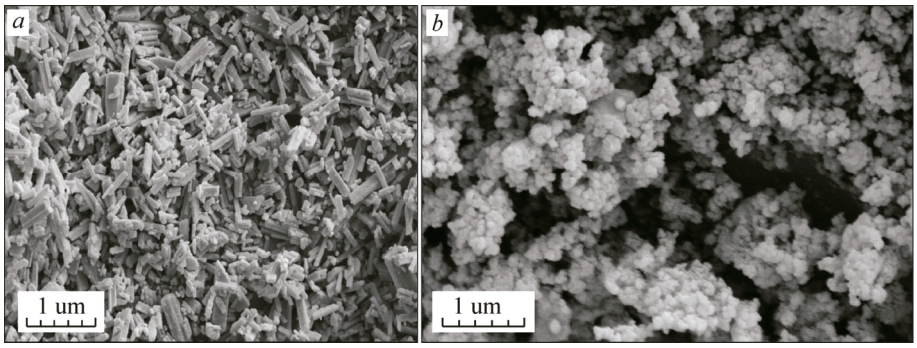

Fig. 5. SEM photographs of nanostructures of compound **1** prepared with the 80 min sonication time in 1:1 methanol: chloroform (*a*) and methanol (*b*)

Concentrations of starting materials. The morphology and particle sizes of the structures depend on the concentrations of initial reagents. Thus, the concentrations of initial materials were changed as an effective parameter in both types of solvents. The reactions were performed with four different concentrations (Table 1).

A comparison between the samples with different concentrations shows different results. In mixed solvents (methanol: chloroform) a decrease in the concentration has a negative effect on the size and distribution of structures. Therefore, the concentrations of starting materials for sample No. 1 were considered as the optimal value. In the methanol solvent high concentrations of initial reagents yielded more agglomerated particles. Thus, particle sizes produced using lower concentrations of the initial reagents (2.5 mmol, sample No. 5) have better morphology than particle sizes produced with other concentrations.

Sonication time. In order to investigate the sonication time as an effective parameter for the size and morphology of the structures, two further experiments were conducted (Table 1, samples Nos. 9 and 10).

With a lower sonication time it seems more agglomeration of particles happened, leading to semi bulk structures. Therefore, it can be concluded that a higher sonication time prevents the particle agglomeration. Hence, a sonication time of 80 min is considered as the optimal value.

Thermal studies. The thermal decomposition behavior of nanosized compound **1** was investigated on heating from ambient temperature to 800 °C (Fig. 6). Compound **1** is stable up to 113 °C. At this temperature, one methanol molecule was evaporated (calc: 8.83 %, obs: 9.01 %) with endothermic effects. The experimental mass loss of 18.39 % is consistent with the calculated value of 14.44 % for the elimination of three methyl groups at 297 °C with endothermic effects. At higher temperatures, the decomposition of the compound occurs accompanied by two endothermic effects at 550 °C and 696 °C to ultimately give a solid that appears to be molybdenum(VI) trioxide powder (calc: 40.97 %, observed: 46.05 %).

Preparation of molybdenum trioxide. Depending on the experimental conditions, different MoO_3 polymorphs can be obtained. To prepare molybdenum trioxide nanoparticles, samples of prepared compound **1** under optimal conditions were calcinated at 700 °C for 4 h. A white powder was obtained. The MoO_3 materials prepared after calcination were characterized by X-ray diffraction and FT-IR measurements. Fig. 7 shows the X-ray diffraction (XRD) spectra of the powders. The white powder is crystalline and corresponds to α-MoO_3 (JCPDF 37-519).

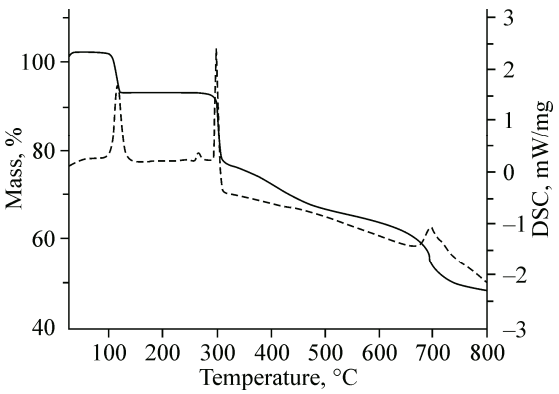

Fig. 6. Thermal behavior of compound **1**

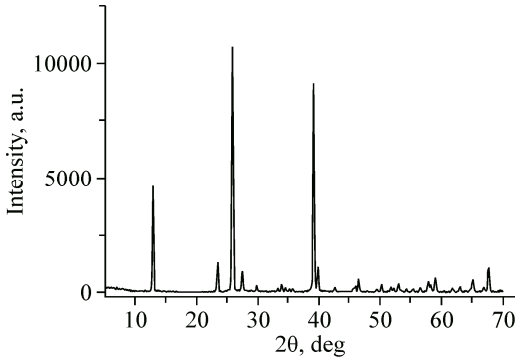

Fig. 7. XRD pattern of MoO_3 nanoparticles prepared by calcination of compound **1** at 700 °C

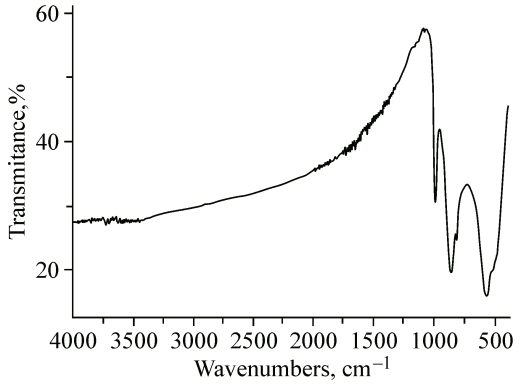

Fig. 8. FT-IR absorption spectra of α-MoO_3

The analysis of the XRD pattern reveals that the MoO_3 sample crystallizes in the orthorhombic symmetry with the *Pbnm* space group. According to Bragg′s law, $d_{hkl} = \frac{\lambda}{2\sin\theta}$, where d_{hkl} and $\lambda = 1.54056$ Å is the interplanar spacing and the used X-ray wavelength. The lattice parameters $a = 3.963(1)$, $b = 13.856(0)$, $c = 3.696(6)$ Å and the unit cell volume $V = 202.9(85)$ Å^3 are determined. The sharp and intense peaks in the XRD pattern of the product demonstrate good crystallinity of MoO_3 nanoparticles. The crystallite size of the molybdenum residual at 700 °C was estimated from the full width at half maximum (FWHM) of the characteristic XRD peaks using Debye—Scherrere equation (1).

$$D = K\lambda / \beta\mathrm{Cos}\theta, \quad (1)$$

where D is the particle (crystallite) size; K is a constant (0.94 for the Cu grid); λ is the X-ray wavelength (1.54056 Å); θ is the Bragg diffraction angle, and β is the integral peak width. The particle size was calculated according to the highest intensity value. The particle size was estimated to be 20 nm, i.e. within the nanoscale range and in agreement with the SEM results.

Fig. 8 exhibits the FT-IR spectra of MoO_3 powders. Broad bands on the low energy side of the FT-IR spectrum below 1000 cm^{-1} are due to the molybdenum oxide network. Two main regions appear in the spectra of MoO_3 compounds that are vibrations at 1000—600 and 600—400 cm^{-1}. The band at 550—600 cm^{-1} is typical of the vibration of the Mo_2O_2 entity formed by edge sharing MoO_6 polyhedra building the orthorhombic α-MoO_3 structure. The band at 995 cm^{-1} is characteristic of the vibration of the Mo=O terminal bond [31, 32]. The dominant band at 860 cm^{-1} is associated with the vibration of Mo—O—Mo bridging bonds [33—35].

SEM images of the residues obtained by direct calcination of the nanostructures of compound **1** at 700 °C shows the formation of MoO_3 nanoparticles (Fig. 9). As seen in Fig. 9, calcination of the compound obtained by the solvothermal method and sample No. 1 (sonochemical method) yielded nanoparticles of molybdenum trioxide with diameters of 30—40 and 50—60 nm respectively. Calcination of sample No. 5 (sonochemical method) yielded a mixture of plates, rods, and nanoscale particles while the use of the bulk complex, prepared by reflux, as a precursor afforded micro structures of MoO_3 accompanied by nanoparticles.

CONCLUSIONS

Methanol {2-[(2-hydroxy-1,1-dimethyl-ethylimino)-methyl]phenolato}dioxidomolybdenum(VI) complex (**1**) was synthesized by sonochemical irradiation and the solvothermal method and their crystal structures were compared. Compound **1** was characterized by elemental analysis, powder XRD, FT-IR and UV-Vis spectroscopy, TG and DSC analyses. To prepare compound **1**, two methods were used: sonochemical and solvothermal. In the sonochemical method some parameters such as the type of the solvent, concentrations of initial reagents, and the sonication time were examined and their

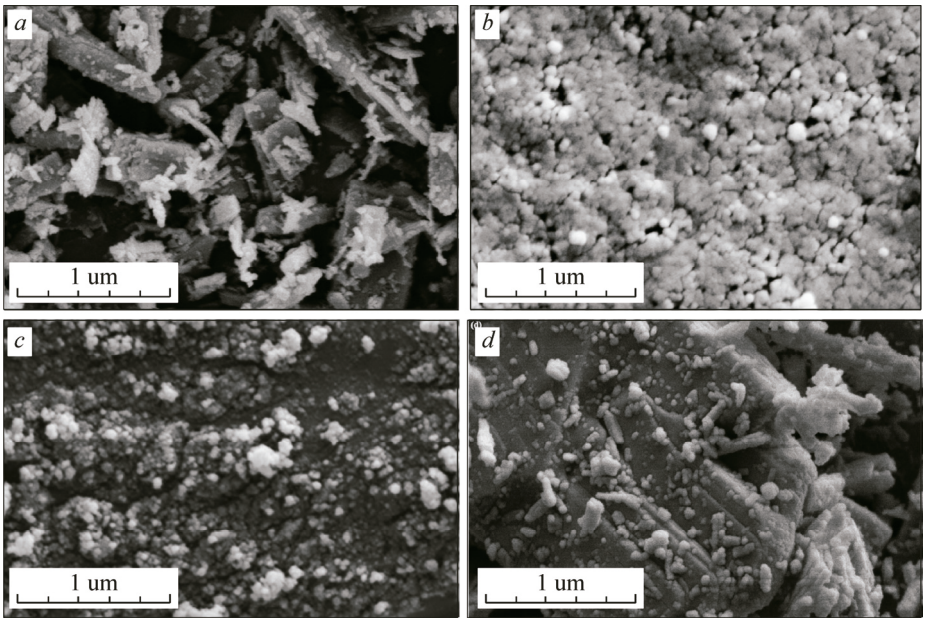

Fig. 9. SEM image of MoO_3 nanoparticles obtained by calcination of compound **1** prepared by the ultrasonic process (sample No. 1 (*a*) and sample No. 5 (*b*)), the solvothermal method (*c*), and the bulk complex at 700 °C(*d*)

effects on the shape, morphology, and size of the structures were investigated. The type of the solvent affected the shape of compound **1**, in the 1:1 mixture of methanol and chloroform some nanorods were obtained, meanwhile in methanol nanoparticles of compound **1** were obtained. The results show that the morphology and particle sizes of the structures depend on the concentrations of initial reagents and the ultrasound irradiation time. The optimal size of compound **1** was obtained at a concentration of 5 mmol in methanol: chloroform and 2.5 mmol in methanol. A decrease in the sonication time led to a greater agglomeration in both types of solvents. Calcination of compound **1** at 700 °C in a furnace and static air atmosphere for 4 h yields molybdenum trioxide nanoparticles.

Support of this investigation by Vali-e-Asr University of Rafsanjan is gratefully acknowledged.

REFERENCES

1. *Bagherzadeh M., Latifi R., Tahsini L., Amani V., Ellern A., Keith Woo L.* // Polyhedron. – 2009. – **28**. – P. 2517.
2. *Barriere F.* // Coord. Chem. Rev. – 2003. – **71**. – P. 236.
3. *Inscore F.E., Knottenbelt S.Z., Rubie N.D., Joshi H.K., Kirk M.L., Enemark J.H.* // Inorg. Chem. – 2006. – **45**. – P. 967.
4. *Romao M.J.* // Dalton Trans. – 2009. – **21**. – P. 4053.
5. *Mosch-Zanetti N.C., Wurm D., Volpe M., Lyashenko G., Harum B., Belaj F., Baumgartner J.* // Inorg. Chem. – 2010. – **49**. – P. 8914.
6. *Schachner J.R.A., Traar P., Sala C., Melcher M., Harum B.N., Sax A.F., Volpe M., Belaj F., Mosch-Zanetti N.C.* // Inorg. Chem. – 2012. – **51**. – P. 7642.
7. *Głowiak T., Jerzykiewicz L., Sobczak J.M., Ziołkowski J.J.* // Inorg. Chim. Acta. – 2003. – **356**. – P. 387.
8. *Sah A.K., Rao C.P., Saarenketo P.K., Wegelius E.K., Kolehmainen E., Rissanen K.* // Eur. J. Inorg. Chem. – 2001. – **2001**. – P. 2773.
9. *Rao C.P., Sreedhara A., Rao P.V., Verghese M.B., Rissanen K., Kolehmainen E., Lokanath N.K., Sridhar M.A., Prasad J.S.* // J. Chem. Soc., Dalton Trans. – 1998. – P. 2383.
10. *Nugent W.A., Mayer J.M.* Metal—Ligand Multiple Bonds. – New York: Wiley-Interscience, 1988.
11. *Tsuruoka T., Furukawa S., Takashima Y., Yoshida K., Isoda S., Kitagawa S.* // Angew. Chem. Int. Ed. – 2009. – **48**. – P. 4739.

12. *Guo H., Zhu Y., Qiu S., Lercher J.A., Zhang H.* // Adv. Mater. – 2010. – **22**. – P. 4190.
13. *Suslick K.S., Choe S.-B., Cichowlas A.A., Grinstaff M.W.* // Nature. – 1991. – **353**. – P. 414.
14. *Ranjbar Z.R., Morsali A.* // J. Mol. Struct. – 2009. – **936**. – P. 206.
15. *Masoomi M.Y., Mahmoudi G., Morsali A.* // J. Coord. Chem. – 2010. – **63**. – P. 1186.
16. *Sadeghzadeh H., Morsali A.* // Ultrason. Sonochem. – 2011. – **18**. – P. 80.
17. *Safarifard V., Morsali A.* // Ultrason. Sonochem. – 2012. – **19**. – P. 300.
18. *Akhbari K., Morsali A.* // J. Organomet. Chem. – 2012. – **700**. – P. 125.
19. *Mason T., Peterson D.* // Pract. Sonochem. – 2002. – **2**. – P. 17.
20. *Camacho-Lopez M.A., Haro-Poniatowski H., Lartundo-Rojas L., Livage J., Julien C.M.* // Mater. Sci. Eng. B. – 2006. – **135**. – P. 88.
21. *Comini E., Yubao L., Bando Y., Sbervglieri G.* // Chem.Phys. Lett. – 2005. – **407**. – P. 368.
22. *Miyata N., Suzuki T., Ohyama R.* // Thin Solid Films. – 1996. – **281/282**. – P. 218.
23. *Guerfi A., Dao L.H.* // J. Electrochem. Soc. – 1989. – **136**. – P. 2435.
24. *Julien C., Yebka B., Nazri G.A.* // Mater. Sci. Eng. B. – 1996. – **38**. – P. 65.
25. *Prasad A.K., Gouma P.I., Kubinski D.J., Visser J.H., Soltis R.F., Schmitz P.J.* // Thin Solid Films. – 2003. – **436**. – P. 46.
26. *Comini E., Faglia G., Sberveglieri G., Cantalini C., Passacantando M., Santucci S., Li Y., Wlodarski W., Qu W.* // Sens. Actuators B. – 2000. – **68**. – P. 168.
27. *Chen G.J.J., McDonald J.W., Newton W.E.* // Inorg. Chem. – 1976. – **15**. – P. 2612.
28. *Mercury* 1.4.1. – Cambridge, UK: Copyright Cambridge Crystallographic Data Centre, 2001—2005.
29. *Liimatainen J., Lehtonen A., Sillanpaa R.* // Polyhedron. – 2000. – **19**. – P. 1133.
30. *Rezaeifard A., Sheikhshoaie I., Monadi N., Alipour M.* // Polyhedron. – 2010. – **29**. – P. 2703.
31. *Kihlborg L.* // Ark. Kemi. – 1963. – **21**. – P. 357.
32. *Segun L., Figlaz M., Cavagnat R., Lassegues J.C.* // Spectrochim. Acta, Part A. – 1995. – **51**. – P. 1323.
33. *Harb F., Gerand B., Nowogrocki G., Figlarz M.* // Solid State Ionics. – 1989. – **32/33**. – P. 84.
34. *Eda K.* // J. Solid State Chem. – 1991. – **95**. – P. 64.
35. *Nazri G.A., Julien C.* // Solid State Ionics. – 1995. – **80**. – P. 271.